Dynamical assessment of physiological systems and states using recurrence plot strategies

CHARLES L. WEBBER, JR., AND JOSEPH P. ZBILUT
Department of Physiology, Loyola University of Chicago, Stritch School of Medicine, Maywood 60153; and Department of Physiology, Rush Medical College, Rush-Presbyterian-Saint Luke's Medical Center, Chicago, Illinois 60612

Webber, Charles L., Jr, and Joseph P. Zbilut. Dynamical assessment of physiological systems and states using recurrence plot strategies. *J. Appl. Physiol.* 76(2): 965–973, 1994.—Physiological systems are best characterized as complex dynamical processes that are continuously subjected to and updated by nonlinear feedforward and feedback inputs. System outputs usually exhibit wide varieties of behaviors due to dynamical interactions between system components, external noise perturbations, and physiological state changes. Complicated interactions occur at a variety of hierarchial levels and involve a number of interacting variables, many of which are unavailable for experimental measurement. In this paper we illustrate how recurrence plots can take single physiological measurements, project them into multidimensional space by embedding procedures, and identify time correlations (recurrences) that are not apparent in the one-dimensional time series. We extend the original description of recurrence plots by computing an array of specific recurrence variables that quantify the deterministic structure and complexity of the plot. We then demonstrate how physiological states can be assessed by making repeated recurrence plot calculations within a window sliding down any physiological dynamic. Unlike other predominant time series techniques, recurrence plot analyses are not limited by data stationarity and size constraints. Pertinent physiological examples from respiratory and skeletal motor systems illustrate the utility of recurrence plots in the diagnosis of nonlinear systems. The methodology is fully applicable to any rhythmical system, whether it be mechanical, electrical, neural, hormonal, chemical, or even spacial.

complex systems; nonlinear dynamics; chaos; determinism; noise; stochasticity; respiration; muscle fatigue; rat

IN GENERAL, physiological systems are inherently rhythmical, time-varying processes that exhibit complex dynamics and state-dependant behaviors. Traditional strategies in the analysis of such complex systems have proceeded along two classic paths. The reductionistic approach has sought to simplify experimental preparations in an attempt to limit the number of operating variables. In neurobiology, for example, reduced preparations with decreased degrees of freedom can be instructive concerning mechanisms of respiratory rhythm generation (4, 9). Alternately, the systems approach has focused attention on integrated outputs as driven by constellations of interconnected variables. Here, sophisticated analytic tools of linear mathematics (e.g., correlation, coherence, and spectral techniques) have proven beneficial in the analysis and diagnosis of living systems. More than mere descriptive analysis, the overarching goal has been to understand complicated output behaviors by the use of theoretical modeling. Classic engineering studies incorporating negative feedback designs, for example, have been very successful in simulating physiological systems, especially the cardiovascular system (16).

Under challenge today are the fundamental assumptions that normal physiological systems are both linear and homeostatic (13, 30). Prompted by important discoveries in theoretical mathematics and experimental physics, new paradigms for the study of biological systems and physiological rhythms suggested about a decade ago (1, 2, 10) are starting to be applied to physiological systems. As a consequence, terms and concepts familiar to nonlinear dynamicists, such as chaos, fractals, and strange attractors, are beginning to appear in the physiological literature with greater frequency (11, 12, 30). Encouraged by early successes, we stand on the verge of comprehending biological rhythms in a new light that may enhance our ability to control systems gone awry (22).

Before applying any mathematical tool to physiological systems, implicit knowledge concerning the specific assumptions of and constraints on linear and nonlinear algorithms must first be fully appreciated. Many algorithms require that input data be stationary and of long length, but physiological systems tend to drift in time due to several factors, including nonlinear feedbacks, external noise influences, and dynamical state changes (31). The stationarity constraint of many mathematical tools is favored by analyzing shorter data sets but often at the forfeiture of resolution and accuracy. Alternately, increasing the size of data strings introduces nonstationarity trending that smears out characteristic peaks in the frequency spectrum (Fourier analysis), yields false estimations of the number of operating variables (correlation dimension calculations), and mistakenly identifies the presence of dynamical chaos (positive Lyapunov exponents) (8). The problem resides not with the excellent nonlinear algorithms extant today (14, 15) but with the unsuitability of the physiological data sets. As Casdagli (5) poignantly points out, the repeated claims for the presence of low-dimensional chaos in numerous physiological systems are simply unwarranted.

The purpose of this modeling paper is to explore and extend the utility of one nonlinear diagnostic tool, the
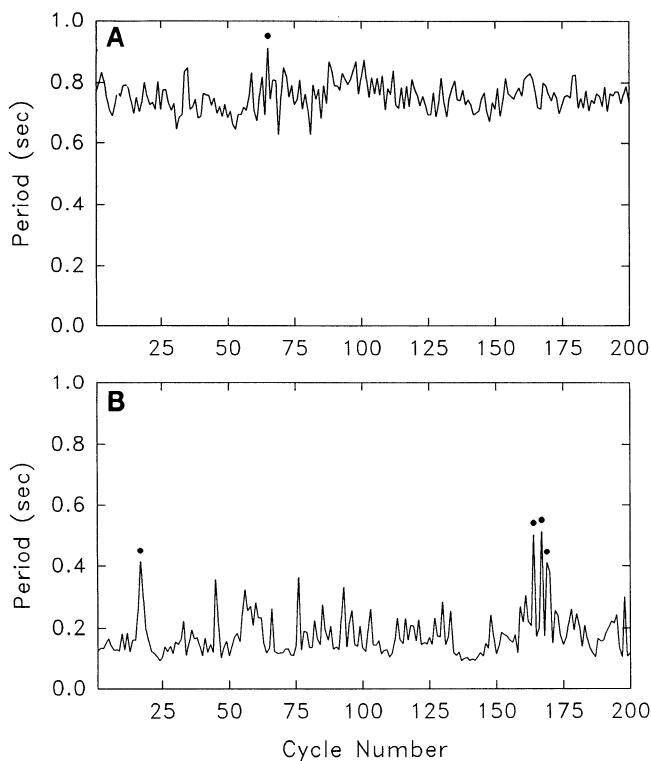
FIG. 1. Respiratory periods from sequential breaths of unanesthetized rat during quiet (A) and active (B) breathing. Respiratory patterns were recorded (500-Hz digitization) as fluctuations in pressure from balloon implanted within intrathoracic space. Periods were defined as time from 1 end inspiration to next (2-ms resolution). Mean periods for quiet and active states were different (0.75 vs. 0.17 s), but their SDs were similar (0.05 and 0.07 s). Also, spectral coherence of 2 signals over frequency range from 0.2 to 11 Hz was relatively high (0.572). This indicates that 2 states cannot be distinguished on basis of their frequency components. Individual breaths beyond 3 SDs of mean periods are marked (●).

recurrence plot, in assessing physiological systems and states. This graphical method, first introduced in the physics literature by Eckmann et al. (7), was originally designed to locate recurring patterns (hidden rhythms) and nonstationarities (drifts) in experimental data sets. Because recurrence plots impose no rigid constraints on data set size, stationarity, or statistical distribution, we hypothesized that this technique might be ideal for physiological data. For example, even when the characteristic times of the dynamical system under study exceed the data set length, meaningful results can still be obtained. Although supposed evidence for deterministic chaos in the breathing patterns of rats (25) and humans (6) has been found by using dimension estimations, our goal was not to search for chaos and reconstruct attractors per se. Rather, we wanted to exploit recurrence plot methodologies to reveal dynamical behaviors not obvious in the fundamental time series and not detected by standard linear techniques (19, 28, 29, 32, 33).

RECURRENCE PLOTS OF PHYSIOLOGICAL SYSTEMS

Breathing patterns of unrestrained rats were recorded by monitoring pressures in balloons placed within the intrathoracic space (28). The duration of individual respiratory cycles were computed as the time between maximum negative pressures in the intrapleural space. Figure 1 shows the typical patterns of 200 sequential respiratory

periods for both quiet breathing (A) and active breathing (B). Quiet breathing was observed when the rat was undisturbed, but active breathing with rapid sniffing was incited by the presence of a second intruder rat. With the exception of mean periods (0.75 vs. 0.17 s), quiet and active patterns possess remarkably similar characteristics in the time and frequency domains. Not only are their standard deviations equivalent (0.05 and 0.07 s), but the two patterns share a relatively strong spectral coherence of 0.572, signifying that their frequency (f) components are comparable over the range from 0.2 to 11 Hz. In addition, both breathing states possess similar $1/f$ scalings ($1/f^{1.7}$ and $1/f^{1.5}$), indicating that the distributions of periods during active and quiet breathing have comparable fractal structures (23).

Differences between quiet and active periods become readily apparent when the two respiratory dynamics are subjected to recurrence plot analysis as shown in Fig. 2. Recurrent points are denoted by darkened pixels located at specific I,J coordinates (sequential cycles). Each family of pixels forms characteristic patterns on two halves (triangles) of the square field that are symmetrical across the central upward diagonal (line of identity). Insofar as the recurrent patterns are more structured for quiet breathing (Fig. 2A) than for active breathing (Fig. 2B), this shows that the time correlation patterns are more complex for the quiet state. This notion is explored in greater detail in RECURRENCE PLOTS OF MATHEMATICAL SYSTEMS.

The first key to understanding recurrence plots is to become acquainted with the rules for darkening pixels at appropriate I,J coordinates. Although we discuss the mathematical theory of recurrences as well as their procedural implementation in other publications (28, 32), an overview is fully appropriate for our present purposes. Systems usually exhibit complex outputs because they possess multiple variables that are interconnected by nonlinear feedbacks. Ideally, it would be sufficient to record from all participant variables to draw conclusions on the system of interest. Pragmatically, this is seldom feasible. However, by employing embedding techniques it is possible to reconstruct a constellation of surrogate variables from a single observed variable (15), in our case, respiratory periods between intrapleural pressure excursions. This mathematical procedure is called embedding in N-dimensional Euclidean space. For our rat data we embedded in 10-dimensional space, leaving room for up to 10 operating variables as contributing to the single observed output variable (respiratory periods). Embedding was accomplished by computing Euclidean norms (vectors) from strings of 10 consecutive respiratory periods throughout the designated data set. Resultant vector metrics were indexed and differenced, with two vectors compared at a time in all possible I,J combinations. Points were designated as recurrent whenever the distance between paired vectors was small (below a designated cutoff value). Single recurrent points were plotted as darkened pixels at corresponding I,J coordinates. Repeating this procedure for the entire I,J matrix constructed the whole recurrence plot. Typically, low cutoff values were selected to emphasize vector pairs close in multidimensional space. Vectors compared with themselves ($I = J$) necessarily computed to distances of zero,
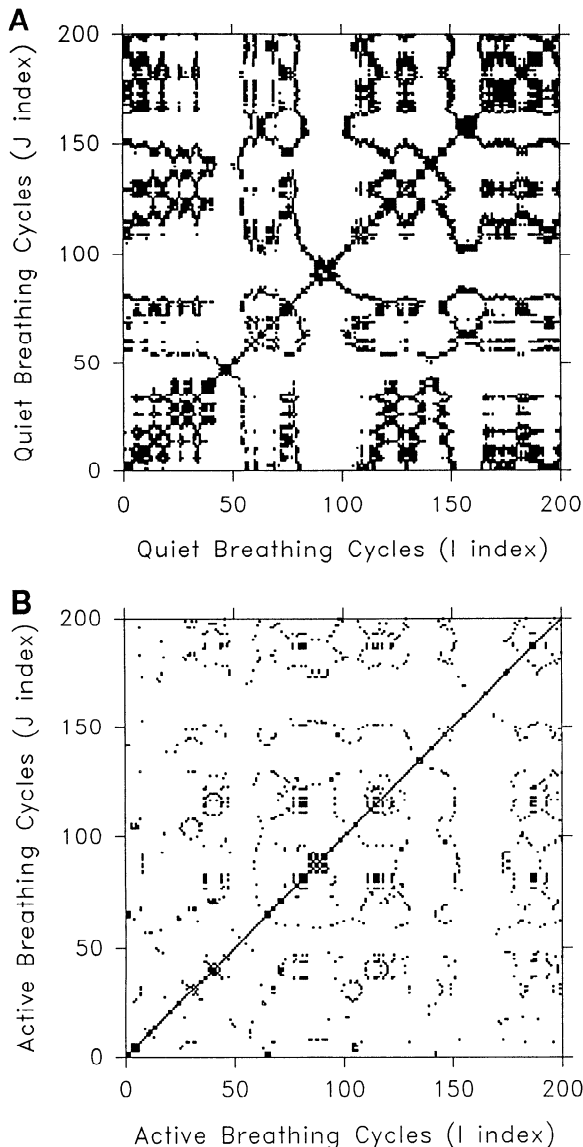
FIG. 2. Recurrence plots derived from quiet (A) and active (B) respiratory periods (see Fig. 1). Recurrent points are designated as blackened pixels that form distinct patterns that are symmetrical across central diagonal (line of identity). Recurrence plots reveal dramatic qualitative differences between quiet (more complex) and active (less complex) states of respiratory system. Computations were performed with following parameter settings: lag = 1 cycle, embedding dimension = 10, cutoff = 1.0 relative unit, and minimum line length = 2 points. Four quantitative measurements were calculated from quiet and active recurrence plots: %recurrence (18.8 vs. 3.4%), %determinism (80.0 vs. 27.5%), ratio (4.248 vs. 8.076), and entropy (2.132 vs. 0.707 bits). See text for further details.

which explains the presence of the strong upward diagonal (line of identity) in all recurrence plots. Eckmann et al. (7) discuss the utility of recurrence plots in revealing subtle time correlations (multidimensional perspective) in otherwise benign time series (1-dimensional perspective).

RECURRENCE PLOTS OF MATHEMATICAL SYSTEMS

The second key to understanding recurrence plots is to appreciate the organization of recurrent points into specific qualitative patterns. One of the better ways to demonstrate this is by closely examining the coupled equations for the Hénon strange attractor (18). This mathematical entity is nothing more than a fully deterministic system consisting of only two interconnected variables with nonlinear feedback (note the squared term)

$$X_{i+1} = Y_i + 1.0 - (1.4X_i^2) \qquad (1)$$

$$Y_{i+1} = 0.3X_i \qquad (2)$$

To the right side of the equal sign the subscript i identifies the iteration number of the current variables. To the left side of the equal sign the subscript $i + 1$ identifies the subsequent iteration number for the updated variables. After each iteration the subscripts are updated ($i = i + 1$), making it possible to compute as many sequential Hénon X and Y values as desired. In practice, X_i and Y_i variables are both initialized to zero, but the first several hundred iterations are discarded before accepting the data. This procedure allows all transients to die away as the dynamic settles down on its strange attractor, a geometrical object controlling the mathematically determined motion of the dynamic. The Hénon attractor, visualized by plotting Y_i as a function of X_i, forms a beautiful double-crescent shape (not illustrated here, but see Refs. 24, 30). Indeed, the identical attractor can be reconstructed from single Hénon variables (X_i vs. X_{i+1} or Y_i vs. Y_{i+1}), demonstrating the generation of surrogate variables by the embedding technique of time delays. The Hénon attractor possesses a fractal dimension of 1.26 (3) with self-similar structures on different scales of magnification (24, 30).

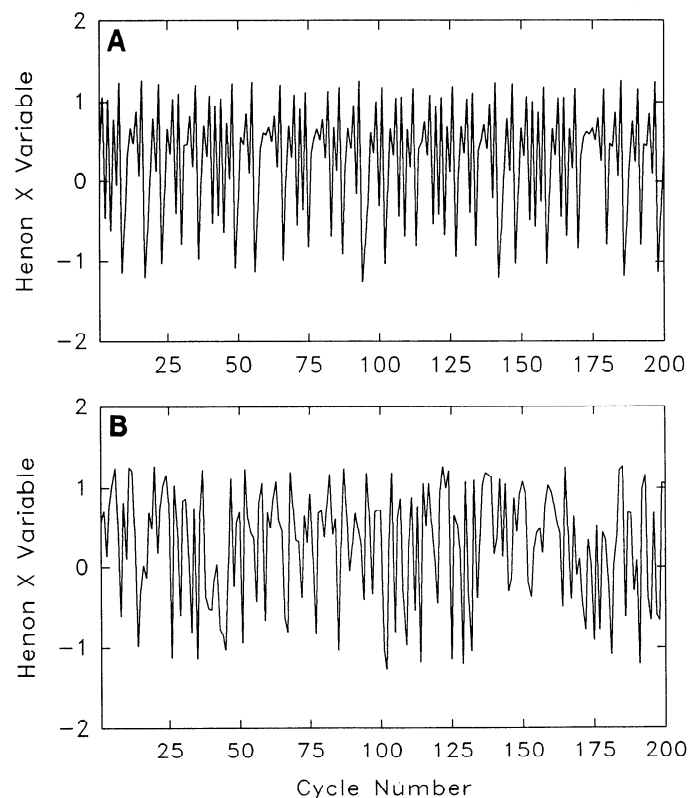In Fig. 3, 200 cycles of the Hénon X variable are plotted

FIG. 3. Iterated values of Hénon X variable before (A) and after (B) shuffling. Means (0.28 and 0.29) and SDs (0.70 and 0.70) for both data sets were the same, but shuffling the sequence 100 times destroyed phasic relationship among Hénon X values. First 1,000 iterations of Hénon system of equations were discarded to remove all transients.

before (A) and after (B) numerical shuffling. Both time series have similar statistics (means, SDs) and both, coincidentally, resemble breathing patterns in the rat. We know that the unshuffled Hénon X variable possesses fully deterministic structure, since it was derived from simple mathematical rules. Shuffling this X variable destroys the phasic time-correlated information in the dynamic, but this is not readily apparent by cursory examination of the time series itself. Indeed, both unshuffled (chaotic) and shuffled (pseudorandom) versions of the same dynamic are rather similar in qualitative and statistical appearance.

Corresponding recurrence plots for the normal Hénon and shuffled Hénon systems are shown in Fig. 4. Recurrent points for the Hénon X variable form distinct short diagonals parallel to, but offset from, the main diagonal among a field of scattered recurrent points. Alternately, recurrence points for the shuffled Hénon X variable are simply distributed in a homogeneous random pattern, signifying that shuffling destroys the deterministic structures in the Hénon system. Although our eyes cannot easily detect differences between the two time series, recurrence plot analysis easily makes the distinction.

We are now prepared to discuss five qualitative features of recurrence plots in a systematic fashion. First, single isolated points are due to chance recurrences in the embedded dynamic. The apparent random scattering of recurrent points is attributed to stochastic (high-dimensional) processes as is seen for the shuffled Hénon system (e.g., Fig. 4B). Second, upward diagonal lines result from strings of vector patterns repeating themselves multiple times down the dynamic. Such patterns are observed for both the Hénon system (Fig. 4A) and the respiratory system in different states (Fig. 2). Mathematically, this type of recurrent structure indicates that the dynamic is visiting the same region of an attractor at different times. Eckmann et al. (7) have shown that the length of these short upward diagonal lines is inversely proportional to the largest positive Lyapunov exponent, one hallmark for chaos in stationary systems. The presence of diagonal lines indicates that deterministic rules are present in the dynamic. In some cases the diagonal lines can be in the downward direction. This occurs whenever the vector sequences at different locations within the dynamic are mirror images of each other. A clear example of this type of patterning can be seen during quiet breathing (Fig. 2A). Third, horizontal and vertical lines result from isolated vectors matching closely with a repeated string of vectors separated in time. Again, this type of recurrent structure is obvious for quiet breathing patterns (Fig. 2A). Fourth, bands of white space in recurrence plots are due to the presence of transients in the time series. Transients are defined as events that lie far outside the normal distribution of values for the otherwise stationary dynamic. For example, during active breathing (Fig. 1B), three of the four marked breaths exceeding three standard deviations above the mean period are tightly clustered (cycles 164, 167, and 169). Embedding these exceedingly long periods in 10-dimensional space results in large vector distances spanning from cycle 155 through cycle 178 and a corresponding broad band of white space over this same range (Fig. 2B).

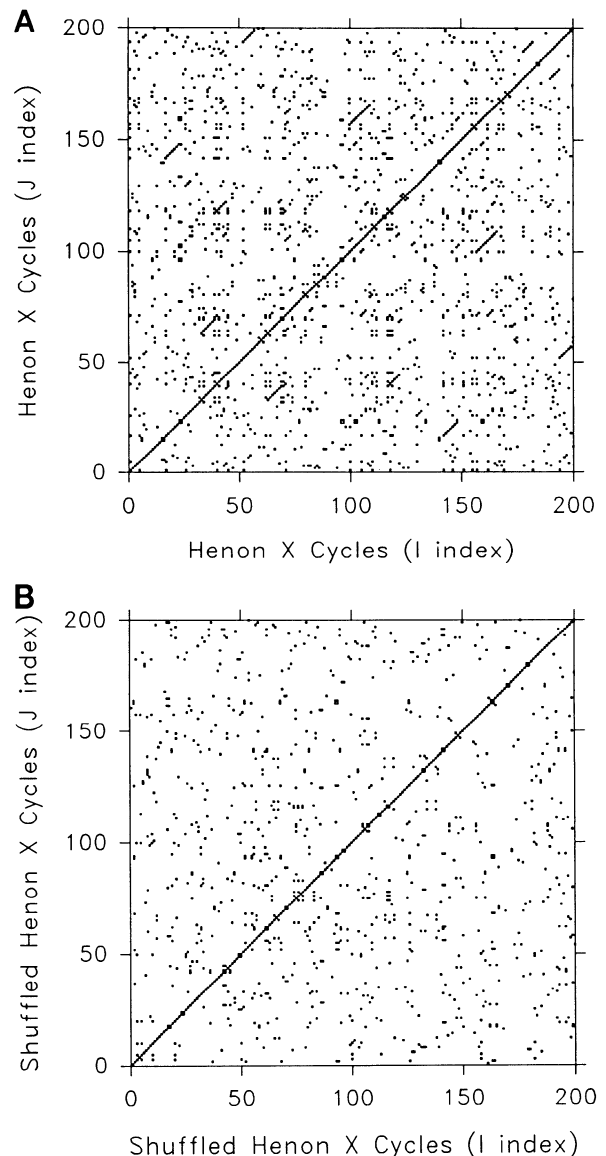FIG. 4. Recurrence plots derived from normal (A) and shuffled (B) versions of Hénon X variable (see Fig. 3). Recurrent points are designated as blackened pixels that form distinct patterns that are symmetrical across central diagonal (line of identity). Recurrence plots reveal dramatic qualitative differences between normal Hénon X variable (more complex) and its shuffled counterpart (less complex). Short upward diagonal line segments representative of determinism in original dynamic are lost after shuffling. Computations were performed with following parameter settings: lag = 1 cycle, embedding dimension = 4, cutoff = 1.0 relative unit, and minimum line length = 2 points. Four quantitative measurements were calculated from normal and shuffled Hénon X recurrence plots: %recurrence (4.1 vs. 2.3%), %determinism (14.6 vs. 4.1%), ratio (3.615 vs. 1.734), and entropy (1.200 vs. 0.503 bits). See text for further details.

Fifth, nonuniform texture or paling of the recurrence plot away from the central diagonal line reflects drifts in the system. None of the four recurrence plots illustrated (Figs. 2 and 4), however, shows any evidence for nonstationarity.

Recurrence plots often contain subtle patterns that are not easily ascertained by qualitative visual inspection. We have solved the problem by defining five quantitative descriptors that emphasize different features of the plot. Understanding the definitions of these specific
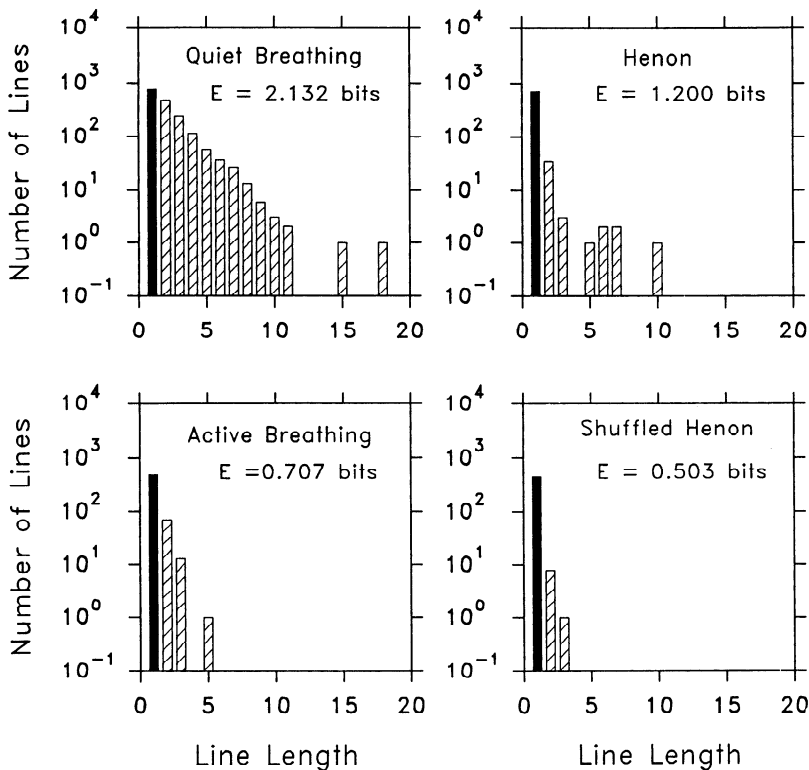
FIG. 5. Computation of Shannon entropy values (E) for recurrence plots of physiological (see Fig. 2) and mathematical (see Fig. 4) systems. Number of upward diagonal line segments of ≥ 2 consecutive points (hatched bars) and isolated points (solid bars) are distributed according to line length. Excluding 1st bin, Shannon E values are computed from all nonzero bin probabilities (P_i) according to $-\Sigma P_i \log_2(P_i)$. Because complexity of recurrence plots is related to magnitude of E, quiet breathing and Hénon system have higher complexities (E = 2.132 and 1.200 bits, respectively) than active breathing and shuffled Hénon system (E = 0.707 and 0.503 bits, respectively). These examples suggest that E fluctuates with changes in physiological state and alterations in phasic information.

markers is the third key to appreciating the power of recurrence plot strategies.

The first variable, percent recurrence, quantifies the percentage of the plot occupied by recurrent points. Mathematically speaking, the number of recurrent points delineates the number of embedded vector pairs near each other in N-dimensional space. Physiologically speaking, this means that embedded processes manifesting periodic dynamics have higher percent recurrence values than other embedded processes characterized by aperiodic dynamics. For example, the quietly breathing rat already introduced had a percent recurrence of 18.8%, but during active breathing this same rat had a percent recurrence of only 3.4% (Fig. 2).

The second variable, percent determinism, quantifies the percentage of recurrent points that form upward diagonal line segments. Lines consist of two or more points that are diagonally adjacent with no intervening white space. This is an extremely important variable, since it distinguishes between recurrent points that are individually dispersed and those that are organized into specific diagonal patterns. The name determinism comes from the fact that diagonal line structures appear in the recurrence plot whenever strings of vectors reoccur further down the dynamic as discussed above. Simply stated, deterministic dynamics repeat themselves. The Hénon system, for example, has 14.6% of its recurrent points in diagonal line structures, but shuffling the dynamic destroys the phasic information and reduces the percent determinism to a mere 4.1% (Fig. 4).

The third variable, entropy, addresses the complexity of recurrence plots by employing principles from Shannon's information theory (27). Line segment lengths (upward diagonals) are counted and distributed over integer bins of a histogram as illustrated in Fig. 5. Usually the

probability for line segments of a particular length decreases sharply as a function of length (logarithmic scale). The Hénon system, however, has significantly longer line segments than its shuffled counterpart (Fig. 4). Likewise, recurrence plots from quiet breathing exhibit longer line segments than those from active breathing patterns (Fig. 2). To quantify these differences, Shannon entropy is computed according to the formula: entropy $= -\Sigma\ P_i \log_2 (P_i)$. Here, P_i represents individual bin probabilities of all nonzero bins greater than or equal to the shortest selected line segment length, in this case two (hatched bars). Because computations are performed with base 2 logarithms, entropy carries the units of bits. Bits, of course, are units of information: the more complex the deterministic structure of the recurrence plot, the larger the number of bits required to represent the dynamic (higher entropy). Thus, because of their broader line segment distributions, entropy values for the Hénon system (E = 1.200 bits) and quiet breathing (E = 2.132 bits) are of higher complexity than the shuffled Hénon (E = 0.503 bits) and active breathing patterns (E = 0.707 bits).

The fourth and fifth variables, ratio and trend, address nonstationarity characteristics in recurrence plots. The ratio variable is defined as the ratio of percent determinism to percent recurrence and is quite useful in the detection of transitions between physiological states. For example, during physiological state transitions, the number of recurrent points (percent recurrence) usually decreases, but the proportion of points in line structures (percent determinism) is less affected. Thus, during physiological transitions, this ratio value increases substantially but settles down again when a new quasi-steady state is achieved. Finally, drift in a dynamical system is characterized by paling of the recurrence plot away from

the central diagonal (7). To quantify drift we compute the percentage of recurrent points in long diagonals parallel to the central line. Percentage values are plotted as a function of distance away from the central diagonal, and a line of best fit is computed. Our trend value is defined as the slope of this line. Systems exhibiting drift have negative or positive trend values; systems free from drift have near zero values.

RECURRENCE PLOTS AND PHYSIOLOGICAL STATE

Lydic (20) has conjectured that physiological studies ignoring organismal state may be likened to experiments in physics disregarding time. The classic approach to the quantification of physiological state has included the computation of moving averages (time domain) and spectral characteristics (frequency domain). During state changes the magnitudes of selected variables are assumed to undergo quantitative modifications that can be associated with the altered mode of the dynamic. However, because the computations of means, standard deviations, and spectral frequency peaks are heavily dependent on system stationarity constraints, it is not surprising that such standard methods are not especially sensitive to physiological state changes.

Because recurrence plots were originally designed to detect hidden rhythms embedded within complex waveforms independent of stationarity restrictions (7), we postulated that our recurrence plot variables would be more sensitive than standard technologies in detecting physiological state changes. Here we discuss two types of physiological experiments supporting our hypothesis, although we surmise that many other illustrations will be forthcoming as recurrence plot strategies are implemented by other investigators on alternate systems.

We take as our first example the detection of breathing pattern alterations during the time course of pentobarbital anesthesia, as shown in Fig. 6. As described previously, respiratory periods were computed from intrapleural pressure traces in rats and plotted as a function of time after the administration of pentobarbital sodium (50 mg/kg body wt ip). The 3,100 respiratory periods comprised 43.8 min of data (Fig. 6A). Before the anesthesia the rat was awake and breathing actively, but subsequent to an intraperitoneal injection of the drug the breathing pattern slowed, supposedly reaching a new steady state. Linear (mean, SD) and nonlinear (recurrence plot) computations were performed within a moving window (200 periods/epoch, 2,892 epochs). The linear metrics closely followed the time series data but did not reveal any subtleties. Thus the mean periods showed an initial rapid increase and then a gradual leveling off to a higher plateau, and the standard deviation periods expressed an initial peaking that soon settled down to an unchanging minimum (Fig. 6B). The nonlinear metrics, on the other hand, possessed much richer dynamics not apparent in the original time series. Variables percent recurrence and percent determinism, for example, showed definite increases during the imposed physiological state change, but the data illustrate interesting oscillations in these measurements even 40 min after the anesthesia was first administered (Fig. 6C). Although we do

not (yet) know the physiological explanation for these oscillations, we conclude that it is inappropriate to assume that a full steady state has been achieved simply on the basis that the respiratory periods seem to have stabilized. When the data are embedded in 10-dimensional space, it becomes obvious that there are continuing underlying oscillations in the dynamic. The induction of these embedded oscillations may be attributable to complicated pharmacodynamics of the drug within the central nervous system and neural networks responsible for rhythmic breathing. Finally, the ratio values are most sensitive to the major state change from active to anesthetized breathing, whereas values of entropy illustrate the waxing and waning complexity of the recurrence plot for the first 20 min after anesthesia (Fig. 6D). Obviously, the embedded dynamics are far richer than the simple time series data imply.

We take as our second example the detection of muscle fatigue during mechanical loading of the human biceps, as shown in Fig. 7. For this experiment, expanded from our first description (26), electromyograms were recorded from the biceps brachii of healthy volunteers. Control recordings of isometric contractions were made for 60 s while the subjects held a 1.4-kg weight (forearm horizontal, elbow at 90°). The mechanical load then was increased to 5.1 kg, and the recording was continued without arm motion until task failure (muscle fatigue). The digitized (1,000 Hz) and band-passed (20–500 Hz) signal was subjected to linear (fast Fourier transform) and nonlinear (recurrence plot) analyses. Skeletal muscle fatigue was indicated by a fall in the center spectral frequency (17) that occurred 74.0 s after placement of the heavy load (Fig. 7A). Recurrence plot analysis on the identical electromyogram signal, however, was able to detect fatigue by the percent determinism variable in the first 48.8 s after loading (Fig. 7C). Similar results were obtained in multiple subjects (Wilcoxon's match-pairs signed-ranks test; $n = 12$; $P < 0.01$), underscoring the practical superiority of recurrence plots in detecting subtle changes in time series missed by less-sensitive techniques. Because the percent recurrence variable remained relatively unaffected during the time course of muscle fatigue (Fig. 7B), the increased percent determinism reveals a reorganization of recurrent points from isolated points into diagonal line assemblies. These pattern changes in recurrence plots are consistent with the synchronization of discharges known to develop in electromyograms during the progression of muscle fatigue (17). One reason muscle fatigue is not as readily detected by spectral analysis is the fact that, by definition, muscle fatigue is a non-steady-state situation. Recurrence plots, alternately, are not stymied by such system drifts, explaining their enhanced sensitivity to changes in the physiological dynamic.

EXPLORATORY DATA ANALYSIS AND HYPOTHESIS TESTING

Physiological systems cannot be explicitly defined in strict mathematical terms, but concepts from nonlinear dynamics are starting to be useful in explaining complex behaviors without a priori knowledge of the dynamical
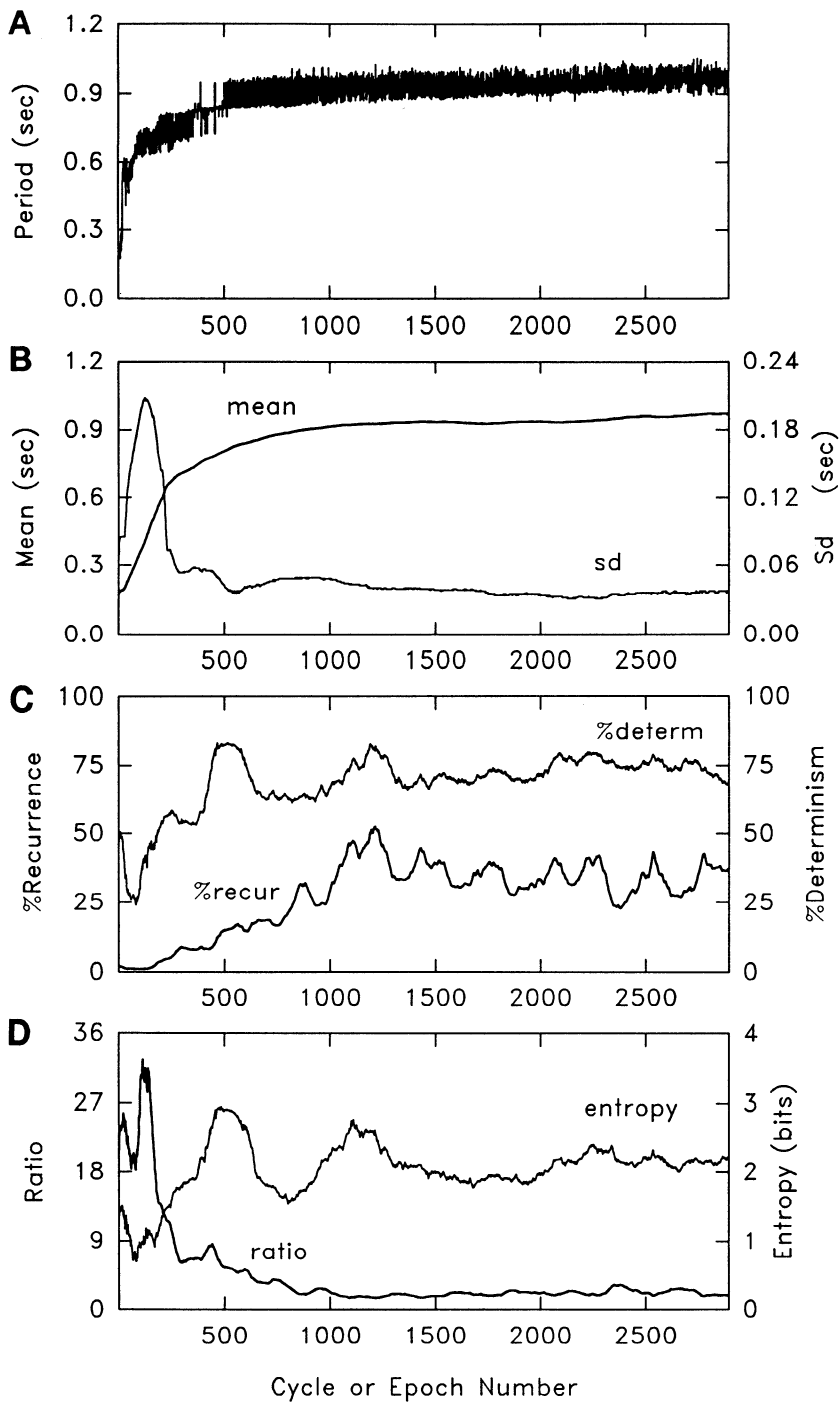
FIG. 6. Linear and nonlinear analyses of breathing pattern transitions during progression from awake to anesthetized state. A total of 3,100 respiratory periods were recorded from rat after intraperitoneal injection of pentobarbital sodium (50 mg/kg body wt) (A). Periods were segmented into 2,892 nonoverlapping epochs, each comprising 200 respiratory cycles. Computations were performed with following parameter settings: lag = 1 cycle, embedding dimension = 10, cutoff = 0.5 relative unit, and minimum line length = 2 points. Linear variables (mean, SD) quickly reached steady-state plateaus after 1,000 epochs (B). Nonlinear variables (%recurrence, %determinism, entropy), however, exhibited sustained oscillations (C and D). Ratio of %recurrence to %determinism showed damped oscillation that reached steady minimum (D). These results indicate that dynamic complexities exist in embedded breathing pattern in 10-dimensional space that are apparently absent in original time series and its standard linear measures.

system of interest. Application of nonlinear algorithms in exploratory data analyses, for example, can provide accurate descriptions of the wide variety of dynamics possible by any system under different conditions (11). Such information is useful despite the lack of mechanistic details of the actual organization of the system. In the future, experimental approaches incorporating nonlinear forecasting methodologies on physiological systems (5) may also become more commonplace.

Complex behaviors and dynamical states of physiological systems can be descriptively analyzed by recurrence plot strategies as discussed in this paper. The power of this new (to physiology) nonlinear tool resides in its ability to resolve subtleties in the original time series by ex-

amining any dynamic in higher dimensional space. We suggest that linear tools not employing embedding strategies and blunted by nonstationarities in the signals under analysis cannot compete successfully with recurrence plot analyses. Thus dynamical changes that are undetectable by standard statistical methodologies may yield under recurrence plot scrutiny. The recurrence plot approach also lends itself to null hypothesis testing, whereby the normal dynamic becomes the null hypothesis (e.g., normal percent recurrence, percent determinism, ratio, entropy values) against which recurrence plot variables of the suspect dynamic can be compared. With the onset of serious disease, for example, it is very important to make an early detection of subtle and detrimental
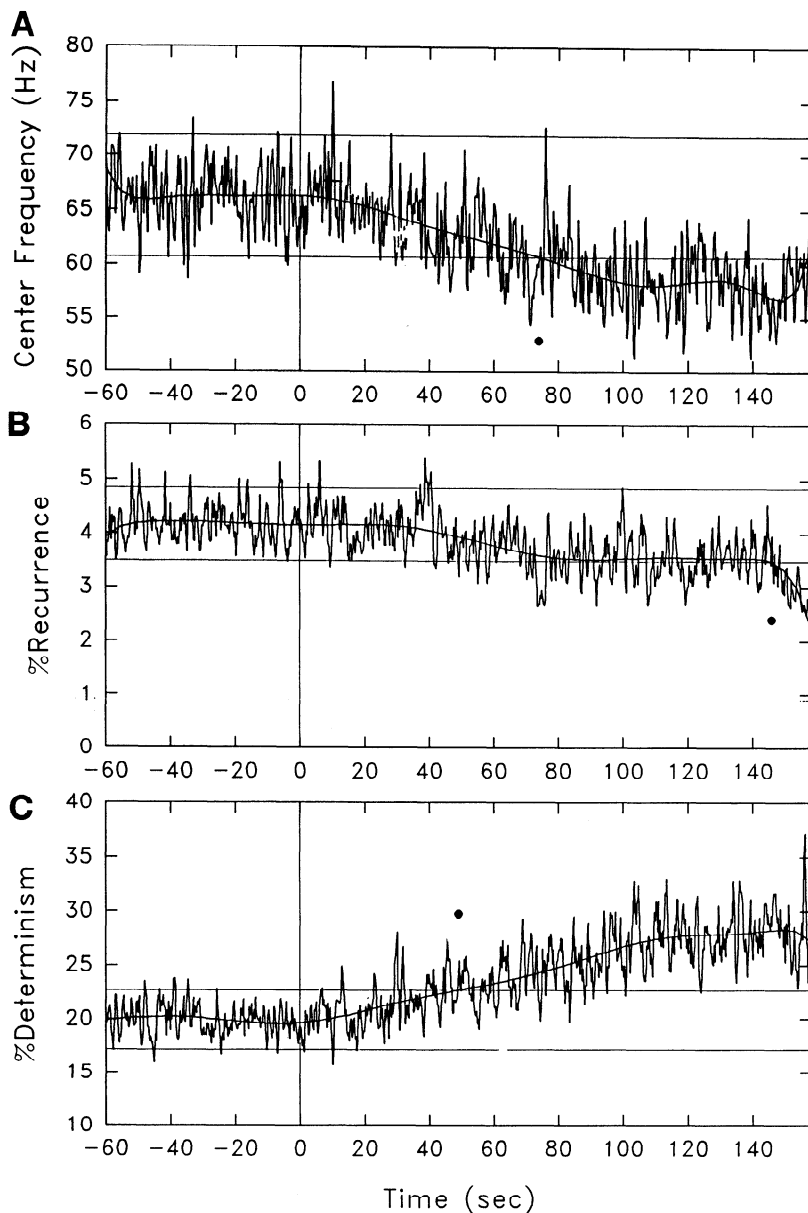
FIG. 7. Linear and nonlinear analyses of biceps electromyographic (EMG) transitions during progression of muscle fatigue. While maintaining their forearms in a horizontal position with elbow bent to 90°, human volunteers were instructed to hold 1.4-kg weight in upward palm for 60 s. At *time 0* (vertical line), load to biceps muscle was increased to 5.1 kg and subjects retained their arm position for as long as possible. EMG was digitized at 1,000 Hz and blocked into 1,024-point epochs. Sequential epochs were offset by 256 points. Computations were performed with following parameter settings: lag = 4 cycles, embedding dimension = 10, cutoff = 2.0 relative units, and minimum line length = 2 points. Confidence limits of 95% were computed for 3 variables during light-load control period (−60 to 0 s), and 10-degree polynomials were passed through computed data. As marked (●), center frequency from spectral analysis (linear measure) detected muscle fatigue 74.0 s after application of heavy load (*A*), but %determinism variable (nonlinear measure) did so in only 48.8 s (*C*). %Recurrence variable (nonlinear measure) remained relatively unaffected by process of fatigue until 145.9 s (*B*). These results illustrate higher sensitivity of recurrence plots over spectral analysis in detecting muscle fatigue.

changes in a dynamical system so that appropriate and timely interventions can be effected. The study of a disease process in its dynamical context may permit effective evaluation of the clinical situation before the actual organic basis for the problem is fully realized (21). Clinical validation of aberrant nonlinear variables, for example, could be studied by conducting retrospective clinical studies on ambulatory recordings from patients at risk of cardiac arrhythmias, epileptic seizures, or sleep apneas. The goal would be to determine the reliability in forecasting whether some dynamical catastrophe is minutes or hours away, giving the physician sufficient time to intervene. Many studies, clinical and experimental, need to be performed to test these important and potentially practical conjectures.

CONCLUSIONS

Among the numerous mathematical tools and nonlinear algorithms available for the study of complex dynami-

cal systems, recurrence plots are ideally suited for physiological data. Unlike other extant instruments, recurrence plots are effective despite the presence of nonstationarities, dynamical noise, system transients, and state changes that typically characterize normal physiological systems. Subtle changes in time series can be detected by pertinent variables that reflect the amount of rule-obeying structure in the dynamic (percent determinism) and the current state of the system (percent recurrence, ratio). Description of the degree of complexity (entropy) of the recurrence plot and system drifts (trend) await further exploration. For the most accurate description of dynamical systems, we recommend that recurrence plots be used judiciously in conjunction with other mathematical tools. One key lesson of nonlinear dynamics is that no single analytic technique in itself is sufficient to characterize a system in its entirety. A battery of tests best suffices.

Dynamical systems theory teaches that complex dynamical behaviors can arise from relatively simple low-

dimensional networks. This implies that reduced experimental preparations, although simpler in structure, may be capable of generating wide varieties of patterns. In any case, data obtained from reductionistic paradigms are not easily extrapolated back to higher integrated levels. Intact, complex physiological systems, on the other hand, probably operate in higher dimensional space with many participant variables. Although it is difficult to estimate the exact dimensions of these systems, recurrence plot strategies can be implemented to study dynamical fluctuations within and between physiological states. Finally, the suggested role of recurrence plots in the diagnosis of dynamical diseases remains an open avenue for productive research. Both animal studies and clinical studies stand to profit from these types of sophisticated approaches.

REFERENCES

1. **Abraham, R. A.** Dynamical models for physiology. *Am. J. Physiol.* 245 (*Regulatory Integrative Comp. Physiol.* 14): R467–R472, 1983.
2. **Basar, E.** Toward a physical approach to integrative physiology. I. Brain dynamics and physical causality. *Am. J. Physiol.* 245 (*Regulatory Integrative Comp. Physiol.* 14): R510–R533, 1983.
3. **Bergé, P., Y. Pomeau, and C. Vidal.** *Order Within Chaos.* New York: Wiley, 1984.
4. **Berger, A. J.** Recent advances in respiratory neurobiology using in vitro methods. *Am. J. Physiol.* 259 (*Lung Cell. Mol. Physiol.* 3): L24–L29, 1990.
5. **Casdagli, M.** *Chaos and Deterministic Versus Stochastic Nonlinear Modeling.* Santa Fe, NM: Santa Fe Institute, 1991. (Santa Fe Inst. Reprint 91–07–029)
6. **Donaldson, G. C.** The chaotic behaviour of resting human respiration. *Respir. Physiol.* 88: 313–321, 1992.
7. **Eckmann, J.-P., S. O. Kamphorst, and D. Ruelle.** Recurrence plots of dynamical systems. *Europhys. Lett.* 4: 973–977, 1987.
8. **Eckmann, J.-P., and D. Ruelle.** Fundamental limitations for estimating dimensions and Lyapunov exponents in dynamical systems. *Physica D* 56: 185–187, 1992.
9. **Feldman, J. L., J. C. Smith, H. H. Ellenberger, C. A. Connelly, G. Liu, J. J. Greer, A. D. Lindsay, and M. R. Otto.** Neurogenesis of respiratory rhythm and pattern: emerging concepts. *Am. J. Physiol.* 259 (*Regulatory Integrative Comp. Physiol.* 28): R879–R886, 1990.
10. **Garfinkel, A.** A mathematics for physiology. *Am. J. Physiol.* 245 (*Regulatory Integrative Comp. Physiol.* 14): R455–R466, 1983.
11. **Glass, L., and M. C. Mackey.** *From Clocks to Chaos.* Princeton, NJ: Princeton Univ. Press, 1988.
12. **Glenny, R. W., H. T. Robertson, S. Yamashiro, and J. B. Bassingthwaighte.** Applications of fractal analysis to physiology. *J. Appl. Physiol.* 70: 2351–2367, 1991.
13. **Goldberger, A. L.** Is the normal heartbeat chaotic or homeostatic? *News Physiol. Sci.* 6: 87–91, 1991.
14. **Grassberger, P., and I. Procaccia.** Measuring the strangeness of strange attractors. *Physica D* 9: 189–208, 1983
15. **Grassberger, P., T. Schreiber, and C. Schaffrath.** Nonlinear time sequence analysis. *Int. J. Bifurcation Chaos* 1: 521–547, 1991.
16. **Guyton, A. C.** Long-term arterial pressure control: an analysis from animal experiments and computer and graphic models. *Am. J. Physiol.* 259 (*Regulatory Integrative Comp. Physiol.* 28): R865–R877, 1990.
17. **Hägg, G. M.** Interpretation of EMG spectral alterations and alternation indexes at sustained contraction. *J. Appl. Physiol.* 73: 1211–1217, 1992.
18. **Hénon, M.** A two-dimensional mapping with a strange attractor. *Commun. Math. Phys.* 50: 69–77, 1976.
19. **Koebbe, M., and G. Mayer-Kress.** Use of recurrence plots in the analysis of time-series data. In: *Nonlinear Modeling and Forecasting, SFI Studies in the Sciences of Complexity,* edited by M. Casdagli and S. Eubank. Redwood City, CA: Addison Wesley, 1992, p. 361–378.
20. **Lydic, R.** State-dependent aspects of regulatory physiology. *FASEB J.* 1: 6–15, 1987.
21. **Mackey, M. C., and J. G. Milton.** Dynamical diseases. *Ann. NY Acad. Sci.* 504: 16–32, 1987.
22. **Mayer-Kress, G., and A. Hübler.** Time evolution of local complexity measures and aperiodic perturbations of nonlinear dynamical systems. In: *Quantitative Measures of Complex Dynamical Systems,* edited by N. B. Abraham. New York: Plenum, 1989, p. 155–171.
23. **Montroll, E. W., and M. F. Shlesinger.** On $1/f$ noise and other distributions with long tails. *Proc. Natl. Acad. Sci. USA* 79: 3380–3383, 1982.
24. **Ruelle, D.** Strange attractors. *Math. Intel.* 2: 126–137, 1980.
25. **Sammon, M. P., and E. N. Bruce.** Vagal afferent activity increases dynamical dimension of respiration in rats. *J. Appl. Physiol.* 70: 1748–1762, 1991.
26. **Schmidt, M. A., J. M. Walsh, and C. L. Webber, Jr.** Improved detection of muscle fatigue by nonlinear analysis of EMG signals (Abstract). *FASEB J.* 6: A2024, 1992.
27. **Shannon, C. E.** A mathematical theory of information. *Bell Syst. Tech. J.* 27: 379–423, 623–656, 1948.
28. **Webber, C. L., Jr.** Rhythmogenesis of deterministic breathing patterns. In: *Rhythms in Physiological Systems,* edited by H. Haken and H.-P. Koepchen. Berlin: Springer-Verlag, 1991, p. 177–191.
29. **Webber, C. L., Jr., and J. P. Zbilut.** The applicability of chaos theory to rhythmic breathing patterns. In: *Cardiorespiratory and Motor Coordination,* edited by H.-P. Koepchen and T. Huopaniemi. Berlin: Springer-Verlag, 1991, p. 239–247.
30. **West, B. J.** *Fractal Physiology and Chaos in Medicine.* Singapore: World Scientific, 1990.
31. **Zbilut, J. P.** Power laws, transients, attractors, and entropy: possible implications for cardiovascular dynamics. In: *Rhythms in Physiological Systems,* edited by H. Haken and H.-P. Koepchen. Berlin: Springer-Verlag, 1991, p. 139–152.
32. **Zbilut, J. P., M. Koebbe, H. Loeb, and G. Mayer-Kress.** Use of recurrence plots in the analysis of heart beat intervals. In: *Proc. IEEE Computers in Cardiology,* edited by A. Muray and K. L. Ripley. Los Alamitos, CA: IEEE Comput. Soc., 1991, p. 263–266.
33. **Zbilut, J. P., and C. L. Webber, Jr.** Embeddings and delays as derived from quantification of recurrence plots. *Physics Lett. A* 171: 199–203, 1992.